

Besides Bandwidth but Sensing Capability of Optical Fibers

Bo-Kuan Yeh¹, Chien-Hsing Chen², Wei-Te Wu^{1*}, Jaw-Luen Tang²

Ext.7599 weite@mail.npust.edu.tw

¹Department of Biomechatronics Engineering, National Pingtung University of Science and Technology

²Department of Physics, National Chung Cheng University

*Assistant Professor, Department of Biomechatronics Engineering, National Pingtung University of Science and Technology

Due to the flourishing development of the optical communication in recent years, people enjoy more convenient and faster data transferring speed. At optical communication industry, optic fibers are a part of the passive hardware components. Because the optical fiber has more benefits compared with traditional cable in data communication, such as low loss and more suitable for long-distance transmission. Just as the name implies, optic fibers play the core component in the fiber optics sensors. Figure 1⁽¹⁾ shows the structure of the typical optical fiber. The price of optic fiber is cheap and the whole communication industry has reached economic scale. For this reason, the related accessories are very rich and easy to get. It helps to create a new niche optical sensor market upon the above-mentioned benefits.

In optical communication industry, silica based fibers are adopted for transmission. It's because this kind of fiber is more suit at long-distance transmission, unlike polymer fiber with larger transmission loss which is more suit at short-distance transmission. There are two main categories of communication fibers: single mode and multi-mode. The multi-mode communication fiber was used in our studies. Mainly because the multi-mode communication fiber can be easy to couple the light and the energy of light transmitted is more enough in comparison with the single mode communication fiber. Therefore, it's beneficial to judge the sensing signal when sensing is processed.

Optical fiber needs to modify the structure in sensing application areas. There are several kinds of structure to achieve sensing requirements, such as fiber grating sensors, interferometer and trench type fiber optic sensors. According to structure period changes, fiber grating sensors can be divided into two types:

long period fiber grating: the grating period is about 10~100 μm .

fiber Bragg grating: it belongs to short-period grating sensors, it has a grating period less than 10 μm .

Fiber grating sensors are usually fabricated by CO₂ laser direct writing, arc discharge machining, UV laser lithography and femtosecond laser machining to make the fiber core with a period structure called grating. Figure 2 (2) shows the structure. The fiber grating can couple the light transmission in fiber cladding, and this alteration will cause the resonance peak formation. The peak shifts in different surrounding environment. Therefore, we can use the fiber grating to measure the temperature, stress, and refractive index changing by analyzing the peak shift level.

However, the fiber grating needs high accuracy fabrication techniques, traditional machining technique can't fit the accuracy requirement. For example, UV laser machining should be considered the material absorption. CO₂ laser and arc discharge machining have the serious and uncontrollable thermal effect problem. However, the femtosecond laser machining can fit the goal without bad side effects. It can be easily designed to achieve different fiber grating sensors.

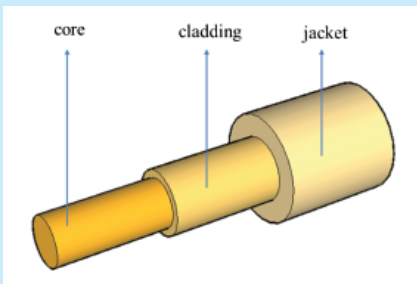


Fig. 1. Structure of the typical optical fiber⁽¹⁾

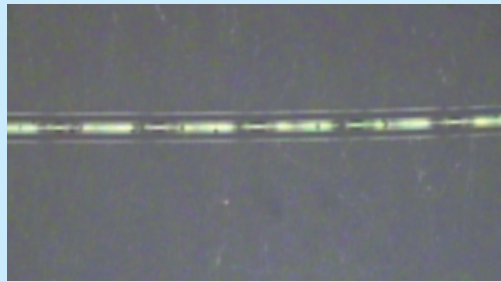


Fig. 2. Diagram of the fiber grating sensor⁽²⁾

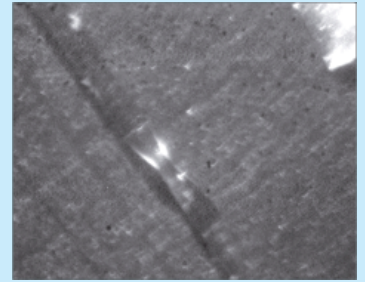


Fig. 3. Diagram of the Mach-Zehnder interferometer⁽³⁾

Interferometer is another kind of optic fiber sensors which is implantation widely. There are two common kinds: Mach-Zehnder interferometer (3): Sensors mainly with a special structure which can cause coherent light with different optical paths, as shown in figure 3. The special structure can divide the light propagates at the fiber core and fiber cladding. In the other side, the similar structure can couple light from different paths into the fiber core forming the interference. Fabry-Perot interferometer (4): Sensors embed a semi-reflective surface which is used to form the interference, as shown in figure 4. When the light propagates through this semi-reflective structure, it forms a penetrating light and reflected light thus causing the different optical paths and forming the interference.

Optical fiber interferometers are mainly fabricated utilization welding method, CO₂ laser direct writing, arc discharge machining and femtosecond laser machining. Among this, welding method is difficult to adjust the parameters, so it easily introduces the structure damage. It is not easy to control the machine parameter by using CO₂ laser and arc discharge machining. The femtosecond laser machining which has the non-linear multi-photon absorption characteristic, it can be fast and easily to achieve the goal. It will be described more detail in the following.

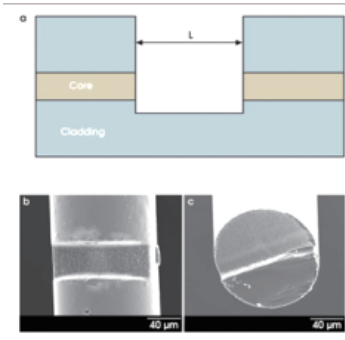


Fig. 4. Diagram of the Fabry-Perot interferometer (4)

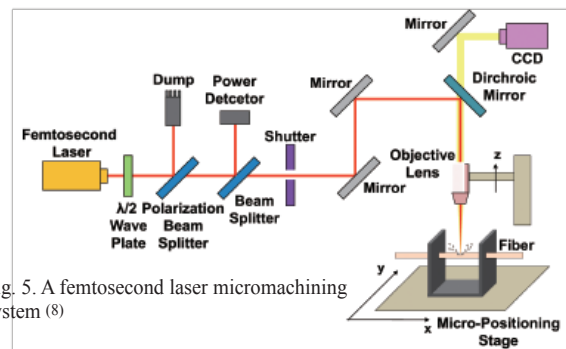


Fig. 5. A femtosecond laser micromachining system (8)

We proposed the concept of trench type fiber optic sensors, in fact, it is the simplest structure. We remove some parts of fiber cladding layer in order to interaction with environment under the basic attenuated total reflection (ATR) principle. Moreover, we can modify functional materials on the exposed fiber core, such as nanoscale gold film and noble metal nanoparticles. Functional materials make fiber optic sensors different sensing scheme; nanoscale gold film inducing surface plasmon resonance (SPR)⁽⁵⁾ and noble metal nanoparticles inducing particle plasmon resonance (PPR)⁽⁶⁻⁷⁾.

In order to fabricate the proposed trench type fiber sensors, we introduce the femtosecond laser machining technique. The most prominent features of the femtosecond laser over conventional long-pulsed laser are ultra short pulse duration and very strong peak power intensity, which can photo-induce the non-linear multi-photon absorption of the material during irradiation interaction. The material vaporizes immediately after absorbing ultra high transient pulse energy from the ultra short pulse of femtosecond laser. It can be used to engrave on transparent, hard and brittle materials very precisely, such as silica-based optical fibers, without inducing any micro cracks and heat affected zone. We just use this mechanism to create one or more exposed structure.

A femtosecond laser micromachining system, as illustrated in figure 5, was used for engraving the trench on the optical fiber. The femtosecond laser was a regenerative amplified mode-locked Ti: sapphire laser with pulse duration of ~120 fs after the compressor, central wavelength at 800 nm, repetition rate of 1 kHz, and maximum pulse energy of ~3.5 mJ. The energy of the linear polarized Gaussian laser beam was adjusted by a rotatable half-wave plate and a polarizing beam splitter (PBS). A certain fraction of the laser beam was split off by a beam splitter (BS) and the laser energy was measured by a power detector. The number of laser shots applied to the sample was controlled by an electromechanical shutter. The laser beam was tightly focused onto the fiber by a 10x objective lens mounted on a Z stage. Minimum spot radius ω_0 is:

$$\omega_0 = (2\lambda f / \pi D) \times M_2 \quad (1)$$

which $\lambda = 800$ nm for the laser wavelength, $f = 20$ mm for the lens focal length, $d = 5$ mm spot diameter for the incident, $M_2 \sim 1.3$ for the laser beam quality. and so can be projected, ω_0 is about $2.5 \mu\text{m}$. The multi-D-shaped trench under fabrication was translated by a computer controlled X-Y micro-positioning stage with error less than $1 \mu\text{m}$. The fabrication process was in situ monitored by a charge-coupled device (CCD)⁽⁸⁾.

Trench type fiber optic sensors which we had manufactured including U-shaped optical fiber which is shown in figure 6⁽⁹⁾. It is a pity that tiny space of the U-shaped trench hard for air escaping and introduces the micro-loading effect. Therefore, we redesigned and scale-up the trench as D-shaped optical fiber for solving the above problem. D-shaped optical fibers are shown in figure 7⁽¹⁰⁾. Moreover, in order to reach the synchronization multitargets sensing, we proposed the concept of multitrench sensors and multiphase sensors for enhancing the mixing in low Re situation. Multiphase sensor is shown in figure 8⁽¹¹⁾.

In order to estimate the performance of fiber-optic sensors, we establish a refractive index sensing experimental, shown in figure 9 is an illustration of the experimental setup for refractive index sensing measurements. The fiber-optic sensing system was used to measure the transmission power of the sensor was consisted of a function generator, a LED light source, a sensing fiber, a microfluidic chip, a photodiode, a lock-in amplifier and a computer for data acquisition. The refractive index and concentration for sucrose solution in the range of 1.333 to 1.403 is shown in table 1⁽¹¹⁾.

The sensing scheme basically is ATR without any functional materials on the exposed fiber core. First, the LED as an excitation light source was modulated by a function generator with a square wave current at a frequency of 1 kHz and a voltage of 3.5 V. Through a fiber collimator, light with a wavelength of 530 nm emitted from the LED was coupled into the optical fiber and was carried through the sensing portion of the D-shaped fiber which was immersed in a sucrose solution of various concentrations. For measurements of transmission power, the ATR signals emitted from the sensing fiber was measured by a photodiode and the light signal was converted into electronic signal in voltage. A lock-in amplifier operating at 1 kHz chopping frequency was used for phase-shift detection of the photodiode output signal and for increasing the voltage scale. Finally, we use the computer to analyze the signal⁽¹⁾. Furthermore, we cooperate with professor Chau (National Chung Cheng University, Department of Chemistry and Biochemistry). Professor Chau's group helps to modify gold nanoparticles in the 6 mm sensing length of the fiber optic sensor, and the sensing scheme changes to the PPR scheme. We summarize the related sensing capabilities of all kinds of trench type fiber optic sensors fabricated by us are shown in table 2⁽⁸⁾.

To sum up we had successful fabricated the several kinds of trench type fiber optic sensors including single U-shaped, single D-shaped, multi-D-shaped, and multiphase D-shaped sensors by using the femtosecond laser machining. After the refractive index experiment, the data shows that sensing resolution is reached 10^{-4} RIU. Therefore, we can put eyes on improving the production rate of the femtosecond laser machining and collocate the rich accessories of mature communication industry, it will be highly promote the developed of optic-fiber sensors. When the time comes, people will discuss not only bandwidth but also resolution, sensitivity or detection limit of the optical fiber!

Reference

- Yeh, B. K., 2011, Investigations of the Fiber-Optics refractive index sensor realized by CO₂ Laser machining. Master Degree Thesis, National Pingtung University of Science and Technology, Department of Biomechatronics Engineering, Pingtung. (in Chinese)
- Chen, C. H., Chen, S. C., Chen, Y. C., Hu, H. T., Wei, T. H., Wu, W. T., Wang, J. N., Tang, J. L., 2009, "Research on laser-induced long-period fiber grating sensor modified with gold nano-rods," The 8th Pacific Rim Conference on Lasers and Electro-Optics, Shanghai.
- Chen, C. H., Chen, Y. C., Wang, J. N., Chau, L. K., Tang, J. L., and Wu, W. T., 2010 "Multimode fiber Mach-Zehnder interferometer for measurement of refractive index", IEEE Sensors 2010 Conference - the 9th Annual IEEE Conference on Sensors, USA. EI
- Hitz, Breck, 2008, "Tiny Fiber Fabry-Perot Created with Femtosecond Pulses," Photonics Spectra, Vol. 42, no. 5, pp. 90-91.
- Homola, J., Yee, S. S., Gauglitz, G., 1999, "Surface plasmon resonance: review," Sensors and Actuators B, Vol. 54, pp. 3-15.
- Salamon, Z., Macleod, H. A., Tollin, G., 1997, "Surface plasmon resonance spectroscopy as a tool for investigating the biochemical and biophysical properties of membrane protein system. II: Applications to biological systems," Biochimica et Biophysica Acta, Vol.1331, pp. 131-152.
- Chau, L. K., Lin, Y. F., Cheng, S. F., Lin, T. J., 2006, "Fiber-optic chemical and biochemical probes based on localized surface plasmon resonance," Sensors and Actuators B, Vol. 113, pp. 100-105.
- Chen, C. H., Hsu, C. Y., Lyu, P. S., Wang, J. N., Chau, L. K., Wu, W. T., Tang, J. L., 2011 "Novel Trench Type Fiber-Optic Sensors Realized by Femtosecond Laser Direct Microstructuring," IPC2011.
- Tsao Tzu-Chien, 2009, Manufacture of Key Components of the Fiber Optics Localized Plasma Resonance Biosensor by Femtosecond Laser, Master Degree Thesis, ational Chung Cheng University, Department Of Mechanical Engineering, ChiaYi. (in Chinese)
- Chen, C. H., Chao, T. C., Li, W. Y., Shen, W. C., Cheng, C. W., Tang, J. L., Chau, L. K., Wu, W. T., 2010, "Novel D-type fiber optic localized plasmon resonance sensor realized by femtosecond laser," Journal of Laser Micro/Nano Engineering, Vol. 5, pp. 1-5.
- Chen, C. H., Weng, T. T., Wang, J. N., Cheng, C. W., Tang, J. L., Chau, L. K., Wu, W. T., 2011, "Novel Multiphase D-shaped Fiber Optic Sensor Realized by Femtosecond Laser Machining," Journal of Laser Micro/Nano Engineering, Vol. 6, pp. 81-86.

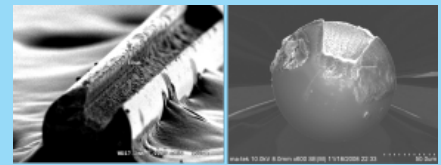


Fig. 6. Single U-shaped optical fiber (9)

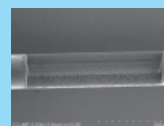


Fig.7. Single D-shaped optical fiber (10)

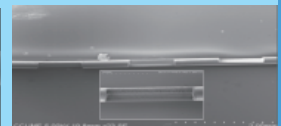


Fig.8. Multiphase D-shaped optical fiber (11)

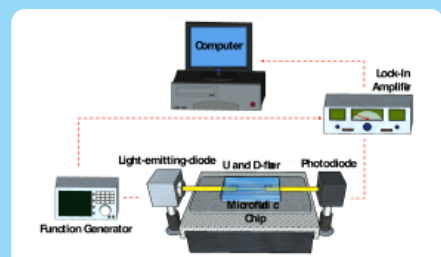


Fig.9. Schematic representation of the experimental setup used to make sensing measurements with the gold nanoparticles-modified U and D-shaped optical fibers (8)

Table 1. Refractive index of sucrose solution with different concentration⁽¹¹⁾

	RIU	Wt %
DI	1.333	0
No.1	1.343	6.8
No.2	1.353	13.25
No.3	1.363	19.45
No.4	1.373	25.4
No.5	1.383	31.05
No.6	1.393	36.55
No.7	1.403	41.7

Table 2. Sensor resolution results of trench type optical fibers (PPR)⁽⁸⁾

	sensing length	slope, m(RIU) ⁻¹	STD, σ	linear correlation, R	resolution, 3 σ m (RIU)
Single U-shaped	6 mm	0.81	1.06×10^{-3}	0.9999	1.06×10^{-3}
Single D-shaped	6 mm	2.90	1.49×10^{-4}	0.9987	1.54×10^{-4}
Multi-D-shaped	6 mm	5.47	5.96×10^{-4}	0.9991	3.27×10^{-4}
Multiphase D-shaped	6 mm	9.62	5.36×10^{-4}	0.9991	1.67×10^{-4}